

Enhancing Digital Cephalic Radiography

S.Venkatakiran¹, C.Kumar²

Associate professor, Department of ECE S.V.P.C.E.T, PUTTUR.

Abstract: We present a new algorithm, called the soft-tissue filter that can make both soft and bone tissue clearly visible in digital cephalic radiographies under a wide range of exposures. It uses a mixture model made up of two Gaussian distributions and one inverted lognormal distribution to analyze the image histogram. The image is clustered in three parts: background, soft tissue, and bone using this model. Improvement in the visibility of both structures is achieved through a local transformation based on gamma correction, stretching, and saturation, which is applied using different parameters for bone and soft-tissue pixels. A processing time of 1 s for 5 M pixel images allows the filter to operate in real time. Although the default value of the filter parameters is adequate for most images, real-time operation allows adjustment to recover under- and overexposed images or to obtain the best quality subjectively. The filter was extensively clinically tested: quantitative and qualitative results are reported here

Index Terms: Digital radiography, histogram-based clustering, image enhancement, local gamma correction,

I. Introduction

CEPHALIC radiographs are widely used by dentists, surgeons, and maxillofacial radiologists for diagnosis, surgical planning, and implant evaluation. Thanks to modern digital radiographic systems, qualitative evaluation becomes possible in real time, as does quantitative measurement and visualization of anatomical features (e.g., nasal spine, chin tip,). Alterations in patient's anatomy and visualization of postoperative aesthetic modifications can be automatically computed and displayed. To take full advantage of these systems, radiograms are usually treated mathematically so as to obtain optimal grey-level coding, using a variety of techniques, which are generally termed Image Enhancement. The challenge arises from the need to achieve an efficient enhancing solution at interactive rates for images that are currently on the order of 5 M Pixels. One of the main challenges in cephalometric radiography is to clearly display both soft and bony tissue in the same image. Establishing ideal exposure parameters for each patient is very difficult, because of the large difference between the absorption coefficients of the two tissues. In practice, the voltage and the amperage of the X-ray tube are estimated so that the full dynamic range of the X-ray detector is used, taking into account the maximum level of radiation deliverable to the patient. As a result, underexposure of bone and overexposure of soft-tissue often occur, leading to images where the bone and soft-tissue pixels take on similar grey levels (GLs) or the background tends to mix with soft tissue. The substructures inside each tissue then cease to be clearly visible, making their identification difficult if not impossible. The procedures aimed at solving these problems are termed soft-tissue filtering. A great deal of work has been devoted to making the different structures more visible by increasing the local contrast at the edge of each image element. Unsharp masking (UM) is one of

the most widely used techniques, . It can be implemented to work in real time, but it enhances only the small features of the image and increases the noise. Moreover, it does not allow recover of underexposed images in which the dynamic range of the bone-tissue regions is compressed: the high frequencies in the corresponding regions have too little amplitude to be clearly visible without adding strong edge artifacts . In an overexposed image, UM identifies the bone structures well but cannot recover the soft-tissue boundary, where the transition between soft tissue and background is smooth and poorly defined (large scale); this is critical, for instance, in the chin tip or nose profile. Scale-space processing has greater capacity to detect features of different sizes but does not completely solve the problems with UM, especially when large structures are present, as in cephalic images. Different solutions are based on morphological analysis through level sets, morphological operators or anisotropic filtering. Although these approaches guarantee greater homogeneity of the GLs within a given feature, the price paid is computational complexity, which leads to a processing time incompatible with real-time operation. Moreover, they suffer from over- or under-enhancement inside the different regions. An alternative approach is based on analyzing the histogram to remap the GLs so that the dynamic range both for soft-tissue regions and for bone-tissue regions is maximized. The most widely used technique in clinical practice is global gamma correction (GC) because it can run in real-time. However, no single value allows clear visibility of both tissues. The usual setting, which is , makes bone structures clearly visible, but soft tissue darkens and tends to mix with the background . Gamma values greater than 1.0 can be profitably used to recover overexposed soft tissue but compress the dynamic range in bone regions. Image equalization (IE) produces results very similar to those obtained with GC, . The inadequacy of these global approaches is obvious.

Therefore, more refined methods that work at a local level have been proposed. Solutions based on local statistics, such as local histogram equalization or homogeneity analysis reframe the task as a globally constrained nonlinear optimization problem, where the remapping of GLs is constrained at different thresholds while maintaining the same ordering. These solutions have the drawback of being computationally intensive and may suffer from over-enhancement. We propose here a novel approach to soft-tissue filtering, which is based on identifying soft and bone tissue in the histogram using an appropriate mixture model composed of two Gaussian distributions and one inverted lognormal distribution. A different local transformation, based on GC, linear stretching, and saturation, is then applied to the pixels belonging to the two tissues. The resulting algorithm was widely tested and was consistently able to produce clear visibility of both tissues. Moreover, its processing time of about one second makes this solution fully compatible with the interactive visualization rate required by clinical use.

Soft-tissue filtering is obtained by five sequential steps. First, a reliable histogram of the image is built by taking out pixels that belong to borders or to the logotype, as well as saturated pixels. The three components of the histogram (background, soft tissue, and bony tissue) are identified through a mixture model and the optimal threshold between soft and bony tissue is identified. This threshold makes it possible to build a map that contains the GC value for each pixel. Finally, this map is smoothed and applied to the original image.

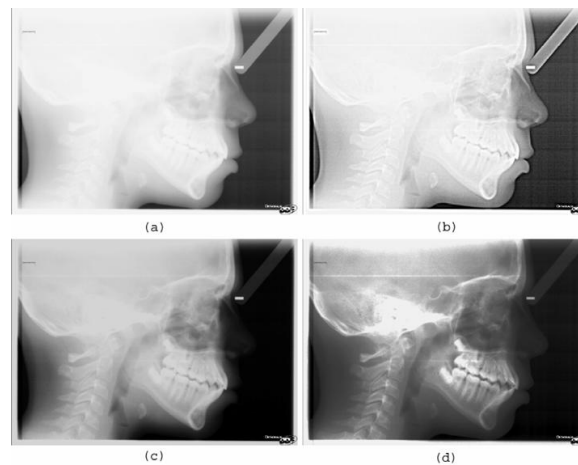


Fig. 1. (a) Typical cephalic radiography, 1871 _ 2605 pixels. (b) Same image treated with UM: the high frequencies are enhanced, but noise is increased, whereas bone is still not clearly visible. (c) Same image after GC, using $\gamma = 0.25$. Although the number of GLs used by the bone pixels (brighter levels) has increased, the range of the dark ones is compressed. (d) Same image after IE. Both GC and IE enhance the bony pixels, but the soft tissue darkens and tends to mix with the background.

II. Histogram Description

The histogram of a cephalic radiographic image has a consistent shape (Fig. 2) with six well-defined peaks. Peak 1 is associated with the pixels that are saturated in the charge-couple device (CCD) sensor, corresponding to GL equal to zero; peaks 2 and 3 represent the image background. The double peak results from automatic exposure control (AEC), which was introduced in the latest generation of radiographic equipment to limit soft-tissue overexposure in the frontal part of the face. Peak 4 is associated with bone structures. It is asymmetrical and shows a steeper slope for the highest GLs. Peak 5 corresponds to pixels at the edge of the CCD sensor, which receive almost no X-rays. Peak 6 is associated with the digital logotype printed on the radiography [corresponding to the maximum GL, equal to L , where L is the number of GLs in the image]. Soft-tissue GLs are spread between peak 2 and peak 4 [Fig. 2(b)]. Under- and overexposed images generate two different histogram populations: as a matter of fact, the bone peak is very high and narrow in underexposed ones, whereas it is lower and broader in overexposed ones [Fig. 2(b)].

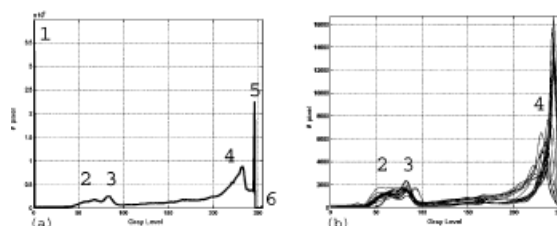
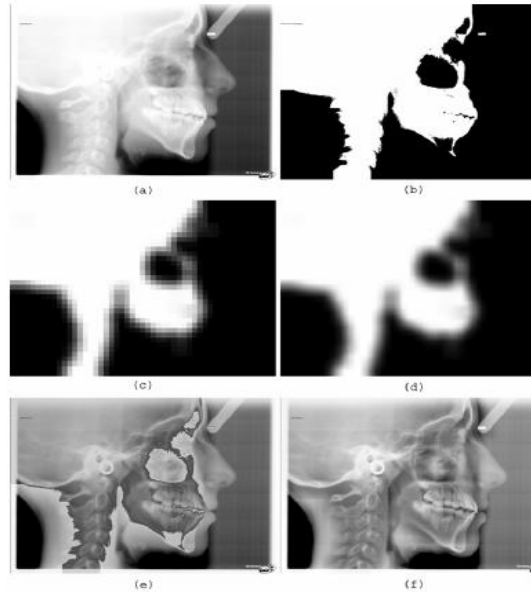


Fig. 2. (a) Typical histogram of a lateral, cephalic radiography shows six marked peaks (see text for a description of the peaks). (b) Histograms of 18 cephalic lateral radiographies after elimination of saturated, edge, and logotype pixels. These were filtered using a moving average filter of size seven

III. Contour, Saturated Pixels and Logotype Elimination

To obtain a reliable computation for the image histogram, first of all, the pixels on the edge of the image are discarded. A boundary frame as large as 5% of the total number of rows and columns is taken out from the image. This is a safe margin to ensure that all the pixels, that were not fully exposed to radiation are discarded. At this point, a working histogram of the image, which we denote as $H_{1F}(x)$

Gamma Map and Local Gamma Correction



(a) Cephalic radiography. (b) Gamma binary field extracted from the same image. (c) Gamma field undersampled and filtered, (d) The final gamma map used for image correction, (e) The image filtered with binary gamma map, artifacts are evident. (f) The result obtained by applying $\Gamma(\cdot)$, using $\gamma = 0.25$, $\gamma = 2.2$, and $TP = N = 1/24$.

At this stage, we could apply pixel-to-pixel GC

$$I'(i, j) = (N_{GL} - 1) \left[\frac{I(i, j)}{N_{GL} - 1} \right]^{\frac{1}{\gamma(i, j)}}$$

as where $I(i, j)$ is the GL of the pixel (i, j) in the original image and $I'(i, j)$ is its value in the image transformed by the gamma $\gamma(i, j)$ value. Specifically, each pixel (i, j) in which $I(i, j) \leq Th_{Bone}$ will be modified by using $\gamma(i, j) = \gamma_{Soft-tissue}$, whereas $\gamma(i, j) = \gamma_{Bone}$ will be used for pixels (i, j) in which $I(i, j) > Th_{Bone}$. Therefore, gamma values have to be smoothed in the spatial domain to avoid strong artifacts. Therefore, we first create a binary gamma map $\Gamma_b(\cdot)$, which contains either the value gamma soft tissue or gamma bone. $\Gamma_b(\cdot)$ has to be spatially filtered to obtain the final gamma map $\Gamma_f(\cdot)$, which will be applied to the image. First $\Gamma_b(\cdot)$ is down-sampled into $\Gamma_d(\cdot)$. Lastly, $\Gamma_f(\cdot)$ is obtained by up sampling $\Gamma_d(\cdot)$ through a bilinear interpolation scheme. To take advantage of the full dynamics of the GLs, linear stretching with saturation is applied to histogram H_{1F} , before local GC. Combining linear stretching with saturation and with local GC yields this final correction formula for each pixel.

IV. Conclusion

One of the main challenges in cephalometric radiography is to clearly display both soft and bony tissue in the same image. Establishing ideal exposure parameters for each patient is very difficult, because of the large difference between the absorption coefficients of the two tissues. In practice, the voltage and the amperage of the X-ray tube are estimated so that the full dynamic range of the X-ray detector is used, taking into account the maximum level of radiation deliverable to the patient. As a result, underexposure of bone and overexposure of soft-tissue often occur, leading to images where the bone and soft-tissue pixels take on similar grey levels (gls) or the background tends to mix with soft tissue. The substructures inside each tissue then cease to be clearly visible, making their identification difficult if not impossible. The procedures aimed at solving these problems are termed soft-tissue filtering.

The filtering algorithm reported here has been widely tested in clinical routines and has proven a powerful tool for visualizing both soft tissue and bone in the same image clearly. Moreover it can be integrated with the latest tools for automatic cephalometric orthodontics. The speed of operation and the intuitive modification of free parameters make it a handy tool for its users. The approach described here can be adapted to all other types of medical images that are characterized by a well-defined multi modal histogram, for which the different tissues have to be displayed clearly in the same image.

References

- [1] R. E. Moyers, *Handbook of Orthodontics*. Chicago, IL: Year Book, 1988
- [2] Y. Chen, K. Cheng, and J. Lin, "Feature subimage extraction for cephalogramlandmarking," in *Proc. IEEE EMBS*, 1998, pp. 1414–1417.
- [3] B. Chanda and D. D. Majumder, *Digital Image Processing and Analysis*. New Delhi, India: Prentice-Hall of India Pvt. Ltd., 2000.
- [4] T.-H. Lin and T. Kao, "Adaptive local contrast enhancement method for medical images displayed on a video monitor," *Med. Eng. Phys.*, vol. 22, pp. 79–87, Mar. 2000.
- [5] D.-C. Chang and W.-R. Wu, "Image contrast enhancement based on a histogram transformation of local standard deviation," *IEEE Trans. Med. Imag.*, vol. 17, no. 8, pp. 518–531, Aug. 1998.